

The Photometric Detection of Transiting Exoplanet WASP-10b

Peter Kalajian
HET 615

Abstract

I have observed the transiting exoplanet WASP-10b (host star: USNO B1.0 1214-0586164) with equipment typical of an advanced amateur astronomer's setup. Over the course of several months, I obtained three transit light curves. Two of these were of high enough quality to submit to the Amateur Exoplanet Archive (AXAWeb). This paper details the process of planning for, obtaining, and processing the data to generate accurate transit light curves of an exoplanet.

1. Introduction

Only one year after the first professional direct photometric transit observation of an exoplanet occurred in 1999 (Charbonneau et al.), a group of amateur observers followed suit with a light curve (Bissinger 2007). At this time, amateurs have contributed light curves for more than 20 exoplanets to the Amateur Exoplanet Archive (AXA).

There are still some exoplanets that are theoretically within the reach of amateurs that have not been observed: WASP-10b (Christian et al. 2008) was one such exoplanet when I began this project. By the time I observed it for the first time on 10 September 2008, one amateur had contributed a light curve, but I contributed the second and third light curves for this object.

WASP-10b was discovered by the SuperWASP group (Pollacco et al. 2006) in 2008 (Christian et al. 2008), using their array of wide field survey cameras. The host star (USNO B1.0 1214-0586164) is a K5-type star in the constellation Pegasus with a $V_{\text{mag}} = 12.7$. Subsequent professional follow-up observations determined that WASP-10b is a hot Jupiter type planet with a mass of $3.06 M_J$ and radius of $1.29 R_J$ and an orbital eccentricity of ~ 0.06 (Christian et al. 2008). This is among the most massive of the currently known transiting exoplanets, and one of the few with a non-circular orbit. Recent dynamical studies (Jackson et al. 2008) show that the orbits of massive closely orbiting planets should circularize after 1 Gyr or so. Adams & Laughlin (2006) have shown that other planets in the system can cause the inner massive planet orbit to cycle through a range of eccentricities on short time scales. By monitoring the transit timing variation (TTV), follow-up observations can detect this eccentricity change.

In many ways, WASP-10b is an excellent target for a first-time exoplanet observer. It orbits around a relatively bright star; there are many similarly bright stars within several arcminutes to use as check stars, and its meridian passage altitude is high enough during the autumn months for Northern Hemisphere observers to eliminate the most egregious effects of atmospheric extinction. In addition, the transit depth of ~ 32 mmags is deep enough that even telescopes of modest aperture (6 to 10 inch) will show the transit dip. TTV observations are essential for detecting other planets in orbit around the host star, and as noted above, WASP-

10b is an ideal candidate for this ongoing TTV program. A diligent amateur who makes regular high-quality WASP-10b LCs may detect evidence for these other planets.

I have observed 3 transits over the course of several months, as noted in §2. I present a detailed analysis of the acquisition, calibration and photometry of the data in §3, and discuss my findings in §4. Appendix 1 is a detailed description of how an amateur might go about observing an exoplanet transit. I hope that others are encouraged to try their hand at catching one of these fascinating periodic events.

2. Observations

I observed 3 transits of WASP-10b: 10 September, 8 October, and 11 October 2008. The field of view for each transit was centered at 23 16 06 +31 26 11 and spanned approximately 11.4' x 8.6' of sky.

A cold front passed to the east of the observatory cleared out the sky less than 30 minutes before the ingress of the 10 September transit. The seeing following a front in Northern New England is always poor and this night was no exception: Stellar FWHM values hovered around 4 arcseconds for the period of the transit. The transparency improved over the first 20 minutes of data collection and steadied out for the rest of the transit. I chose a Johnsons-Cousins R band filter because of the presence of a quarter moon and exposed each frame for 70 seconds to improve the signal to noise ratio, while still keeping the detector in its linear range. The transit period spanned meridian passage, so a meridian flip of the mount interrupted data gathering for several minutes just after the end of ingress. The light curve (LC) for this transit is shown in Figure 9.

The 8 October transit occurred soon after astronomical twilight under excellent photometric conditions. I used a clear filter and exposed for each image for 45 seconds. FWHM values ranged from 3 to 3.7 arcseconds. The transit concluded before meridian passage. See Figure 10 for the LC of this transit.

The 11 October 2008 (R-Band) transit was plagued by intermittent high cirrus clouds that compromised the photometric conditions for the transit. I include the LC of this transit (Figure 11) to illustrate the effects of poor photometric conditions.

The first two transits were submitted to the AXA as the second and third amateur LC contributed for this object.

2.1. Equipment and Software

All observing was done at the Galaxy Quest Observatory, owned by Jacob Gerritsen in Lincolnville, Maine, USA at 44 20.5' N 069 03.8' W using equipment graciously loaned by the owner. The transit observing instrument was a 14" Meade LX200 GPS Schmidt-Cassegrain telescope (MEADEweb) mounted on a Software Bisque Paramount ME (BISQUEweb) with an SBIG AO-8 (SBIGweb) active optics unit between the telescope and the camera

All images were taken with an SBIG ST-2000XM (SBIGweb) anti-blooming camera with an internal TC-237 autoguider chip and cooled to < -20 C. This camera has 7.4-micron square pixels in an 11.8 by 8.9 mm array. Mounted to the LX200, it gives a .81 arcseconds/pixel image scale when binned 2x2.

3. Analysis and Results

I used Maxim D/L (MDLweb) version 4.61 for all image acquisition, reduction, photometry and astrometry in conjunction with the Pinpoint Astrometric Engine (PINPOINTweb). Pinpoint employs the USNO-B1.0 (Monet et al 2003) catalog. All photometry data was subsequently processed using Bruce Gary's (GARYweb) data reduction Excel spreadsheets.

3.1. Image Acquisition and Calibration

Exoplanet transit LCs require accurate timing and accurate photometry. In order to ensure the best possible data, noise must be minimized by applying standard dark and bias frames to the science frames. I created a master dark and bias by median combining 20 of each type immediately following the science run. These were taken at the same chip temperature as the science frame. In addition, I went to great pains to obtain high quality flat frames.

3.1.1. Flat Fields

Ideally, the CCD detector should remain fixed with respect to the stars: each star should affect the same set of pixels for the entire transit. Pixel to pixel variation in sensitivity would be of no concern since the variation of each pixel value over time would be due only to the variation in brightness of the source star. In practice, this is difficult to achieve for a number of reasons. Mount tracking speed, periodic error, and inadequate polar alignment can cause the star to move off a particular set of pixels even with excellent autoguiding. If the target crosses the meridian, a meridian flip is necessary. The use of a tip-tilt optic can compensate for mount errors and seeing scintillation. Since the optic is very light, it can move several times per second in response to changing conditions. My setup includes an SBIG (SBIGweb) AO-8 to accomplish this. Nevertheless, in each of the transits, the AO-8 malfunctioned several times and required reacquisition of the target.

Since these mount issues seem to be inevitable in amateur setups, some sort of flat fielding is necessary to compensate for the pixel-to-pixel variation of the detector response. Obtaining a high-quality noise free flat field image is difficult but essential. I used sky flats exposed at dawn to make a master flat for each of the transits. For the 10 September transit, I obtained a stack of 20 sigma-clip combined dawn sky flats through a diffuser made with two layers of drafting vellum. For the subsequent transits flats were made without the diffuser.

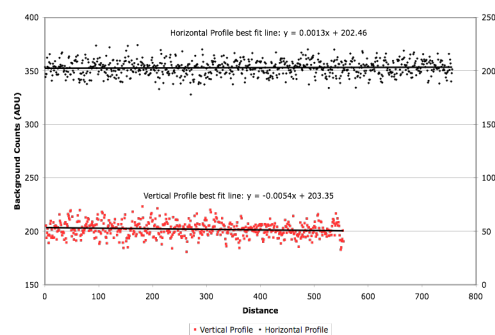


Figure 1. Background pixel values measured along a vertical (red) and horizontal (black) line chosen to miss all sources using MDL's line profile tool.

Figure 1 shows pixel values along horizontal and vertical lines chosen to miss all stars in one image from the Sept 10 transit. There's virtually no slope to the lines of best fit, as would be expected of a quality flat field. Any vignetting would show up as a hump in the line since the middle of the image would be brighter. Any gradients would show up as a slope in the best-fit line. The median pixel value for the background is 203 ADU, and the histogram of values (Figure 2) shows that there are virtually no pixels with values outside of $\pm 2\sigma$ from the mean. That's consistent with a typical Gaussian background noise profile (Howell 2006). I conclude from this analysis that my flat fields are of high quality.

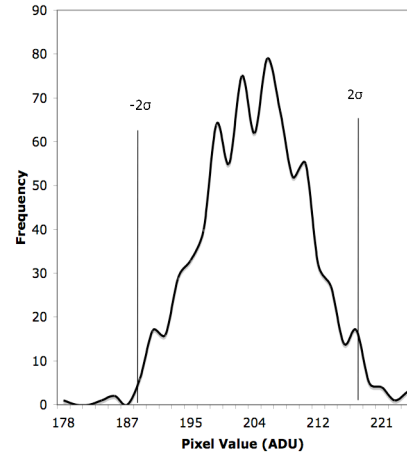


Figure 0. Histogram of pixel values along the horizontal line. Almost all the values lie within 2σ of the median value, typical of a normal background noise distribution.

Both the first and third transit observations spanned the meridian transit, so a meridian flip of the telescope mount interrupted the data acquisition. There were also several instances where the telescope mount slewed off the target and reacquisition was necessary. For both these reasons, both the target star and the check stars were not on the same set of pixels for the entire transit.

3.1.2. Linearity of CCD Detector

Accurate time series photometry of the transit depends on the linearity of the response of the imaging detector to changing light levels. Since the ST-2000 employs anti-blooming gates to eliminate blooming streaks of bright stars, I was concerned about its linearity. In order to test the photometric response of the detector, I aimed the telescope at a 9th magnitude star near the zenith and recorded a series of images with increasing exposure time. By recording the total flux within a photometric aperture and dividing it by the exposure length, I obtained the flux/sec for the star in each frame. Using the median of 5 5-second flux values as the normalization term, I divided the rest of the flux rate values by this term to get a normalized flux rate. This value is plotted against the maximum pixel value within the aperture for each frame in Figure 3. Without employing darks or flats, the detector appears to be quite linear up to maximum pixel values of $\sim 23,000$ ADU. Below this range, the values are within ± 1 percent of linear. I suspect that this error is even less with proper flat fielding and dark correction. Armed with this information, I chose my exposure times to make sure that the maximum pixel value for the target and check stars was below 20,000 ADU.

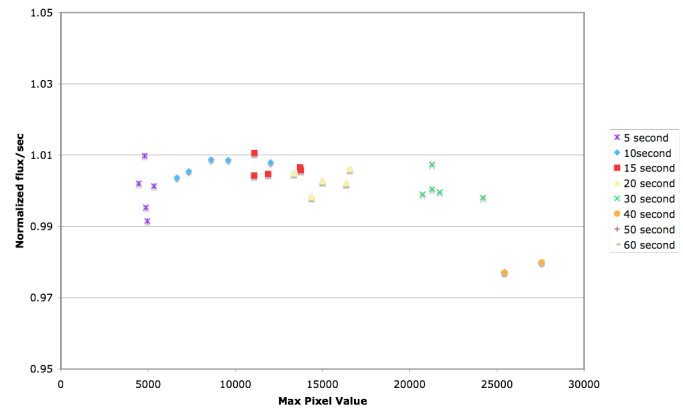


Figure 3. Detector linearity test. The normalized flux rate is linear to $\pm 1\%$ up to maximum pixel values of around 23 kADU.

3.2. Photometry

Artificial star photometry is ideally suited to exoplanet transit measurements. It provides a graphical check on the stability of the photometric atmospheric transparency. Problems like high cirrus clouds, dew on the telescope, changing focus or seeing degradation can all be detected at a glance once an extinction model has been applied to the data.

After image calibration, I aligned each image in MDL and placed a 64 x 64 bit artificial star (available at http://brucegary.net/book_EOA/xls.htm as a plugin for MDL) in the top left corner of each of the aligned images. This serves as the photometric reference star.

MDL includes a photometry tool that allows the user to select a reference star (the artificial star), check stars, and the transiting object to measure. The user can set the photometric aperture, the background annulus and an exclusion radius between the aperture and the background annulus. The background annulus was set to exclude any stars in order to get the best possible background measurement.

After the initial data was plotted, I went back and experimented with different photometric apertures to see how the changes might affect the data. Choosing the size of the aperture is not a trivial exercise. A good starting point is to use FWHM x 3. This will ensure that all the light from the star is in the aperture. This may not be the best aperture, however, because as the aperture gets bigger, so does the noise contribution from the increased number of pixels. Smaller apertures will generate larger signal to noise ratios, but the tradeoff is some loss of pixels that might be from the star but that are outside of the aperture. The best aperture is one that excludes pixels that might have star components but whose value is below the noise level of the background (Howell 2006). See §4.2 for a comparison of various aperture sizes.

The photometry tool measures the magnitude of the object and check stars with respect to the artificial star and outputs these measurements to a comma-delimited text file with the midpoint Julian date and magnitudes for each image. This file serves as the input data for further transit processing. Figure 4 shows the raw magnitude of each frame for the transit star as well as some check stars for the 10 September transit. Notice the large variation in the first dozen images due to the remnants of the cold front. Note also the general downward trend due to extinction at greater airmass.

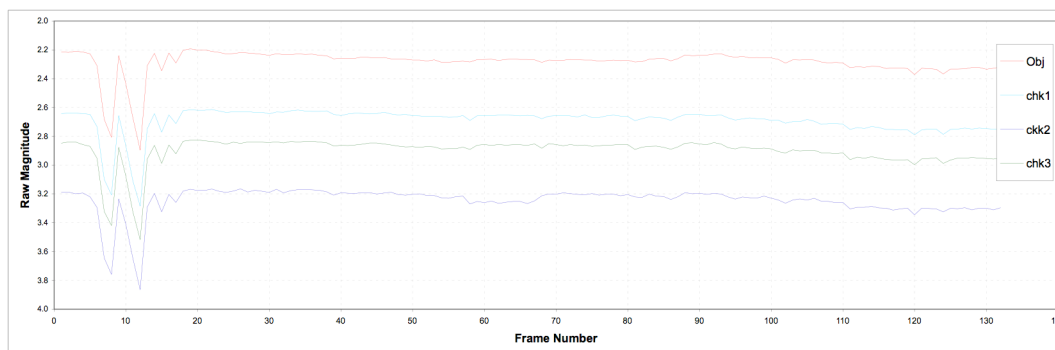


Figure 4. The raw output of MDL's photometry tool for the 10 September transit. WASP10 is shown in red and a few of the check stars are shown as well. The large variation in magnitude in the early frames is due to the last remnants of the passing cold front. From Bruce Gary's Spreadsheet

This raw data needs to be corrected for the extinction due to airmass.

Figure 5 shows a plot of the magnitude of computed from the sum of all well-behaved check star fluxes vs. airmass for the 10 September transit.

In an ideal situation, these points would all lie on a line, the slope of which depended on the extinction characteristics of the atmosphere over the observatory in whatever filter band the images were taken through. The black line is a best-fit linear model of the extinction that will be applied to the transit target based on airmass.

Once the extinction model has been applied, the magnitude of a well-behaved check star should remain constant when plotted against airmass, and changes in the magnitude of the transit star will be due to the transit, not the atmospheric extinction.

Artificial star photometry allows us to go one better, and take care of “extra losses” due to dew, degrading focus, or clouds. This extra loss is calculated by subtracting the average of the check star magnitudes for that image from the median of the average of all the check star values for all images. Figure 6 shows the extra losses and airmass vs. time for the 10 September transit. It is clear that there were some clouds present at the beginning of the science run by looking at the large extra losses. Once the clouds dissipate, the extra losses are remarkably small, another indication of good transparency for the night.

When we apply the extinction correction and the extra loss correction, we can see that the check star magnitudes are now constant (Figure 7). Even large extra losses have been dealt with.

Closer inspection of the graph shows that at least one of the check stars (blue) has a dip in magnitude after the transit. This might be due to the star landing on a different pixel that has not been well calibrated with the flat field, or it might be due to some intrinsic variation in the star’s brightness. Gary (2008) has discovered some variable stars in this way.

Linear modeling of extinction correction seems to be a reasonable approach based on empirical evidence of the constancy of the check star magnitudes over the course of a transit, and the extra loss serves to improve the precision of the measurement.

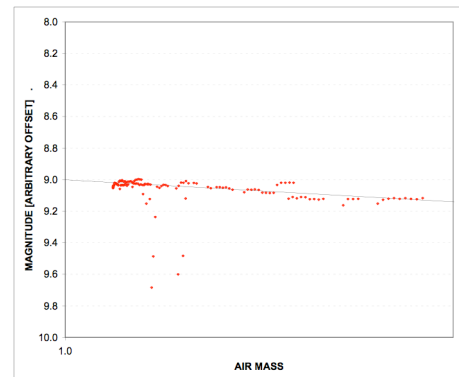


Figure 5. Sum of check star magnitudes vs. airmass for the well behaved check stars for the 10 September transit. Black line is the linear fit model of extinction due to airmass. From Bruce Gary’s spreadsheet

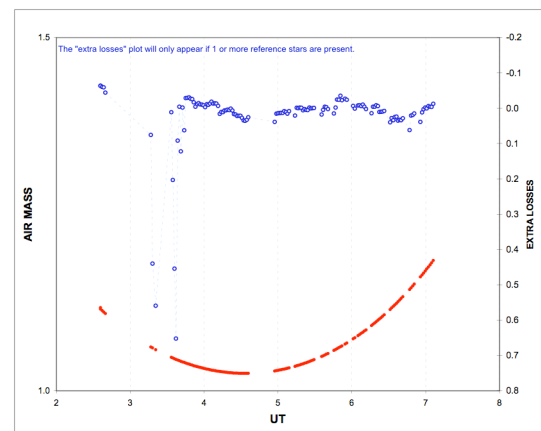


Figure 6. Airmass (red) and Extra Losses (blue) vs. time for the 10 September transit. Note the large extra losses due to the lingering cold front clouds between 3 and 4 UT. From Bruce Gary’s spreadsheet

There are 8 check stars of similar magnitude to the target in the WASP-10 field. Figure 8 shows the field with the R-I color index from the USNO-B1.0 catalog plotted below the stars. These have a range of colors, only two of which are close to that of the transit target. Ideally, we would like to measure check stars with colors close to our target so that the effects of atmospheric extinction will affect all the stars similarly as the zenith distance changes. If the color of check star and target are identical, we need not take into account extinction, because both magnitudes will vary by the same amount as airmass changes. In the case of WASP-10b, some sort of extinction modeling must be done to take into account the varying extinction by color. Even with the extinction model in place, there will be some residual effect due to the difference in color of the check stars and the transit star. This will be discussed in more detail in §4.3.

The final photometric magnitude of the transit star is computed as follows:

$$M_{final} = M_{raw} - C_{ext} \cdot airmass + C_{loss} + ZP$$

Equation 1

Where M_{final} is the adopted magnitude, M_{raw} is the magnitude from MDL, C_{ext} is the extinction correction, C_{loss} is extra losses, and ZP is the zero point magnitude chosen to make the out-of-transit magnitude fit with the accepted magnitude.

3.3. Transit Light Curves

Figures 9-11 show the results of the observations for the three transits. The first two transits were submitted to the AXA and these plots are generated automatically by Bruce Gary's set of software routines (personal communication, Gary 2008). The third suffered from intermittent cirrus clouds and was not submitted to the archive for this reason.

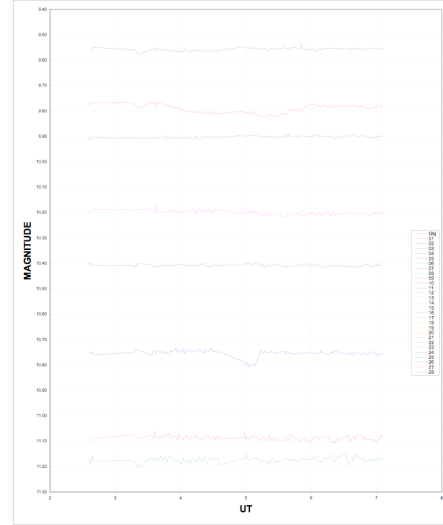


Figure 7. Transit (red) and check star magnitude after correction for extinction and extra losses. Note the dip in the blue check star magnitude after the meridian flip. From Bruce Gary's spreadsheet.

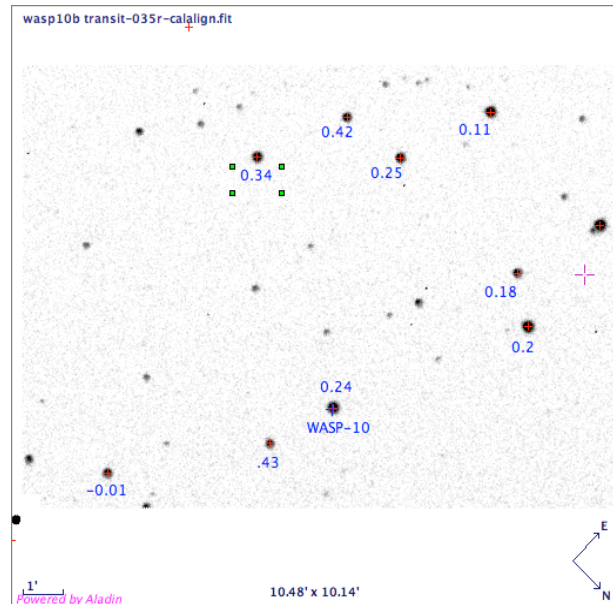


Figure 8. The WASP-10 Field. The USNO B1.0 R-I color index of each check star is plotted below the star. Image manipulated using Aladin (Bonnarel et al. 2000).

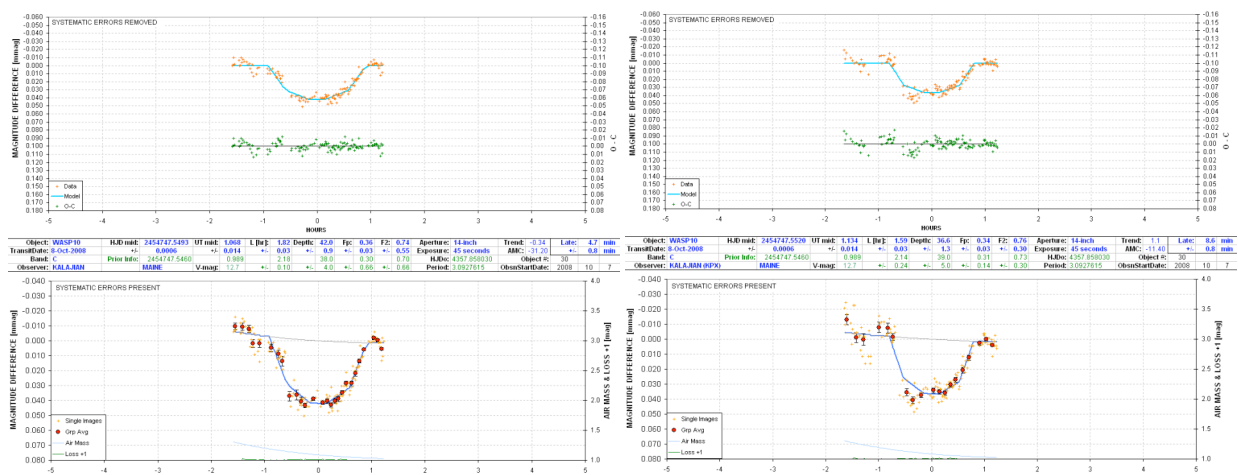
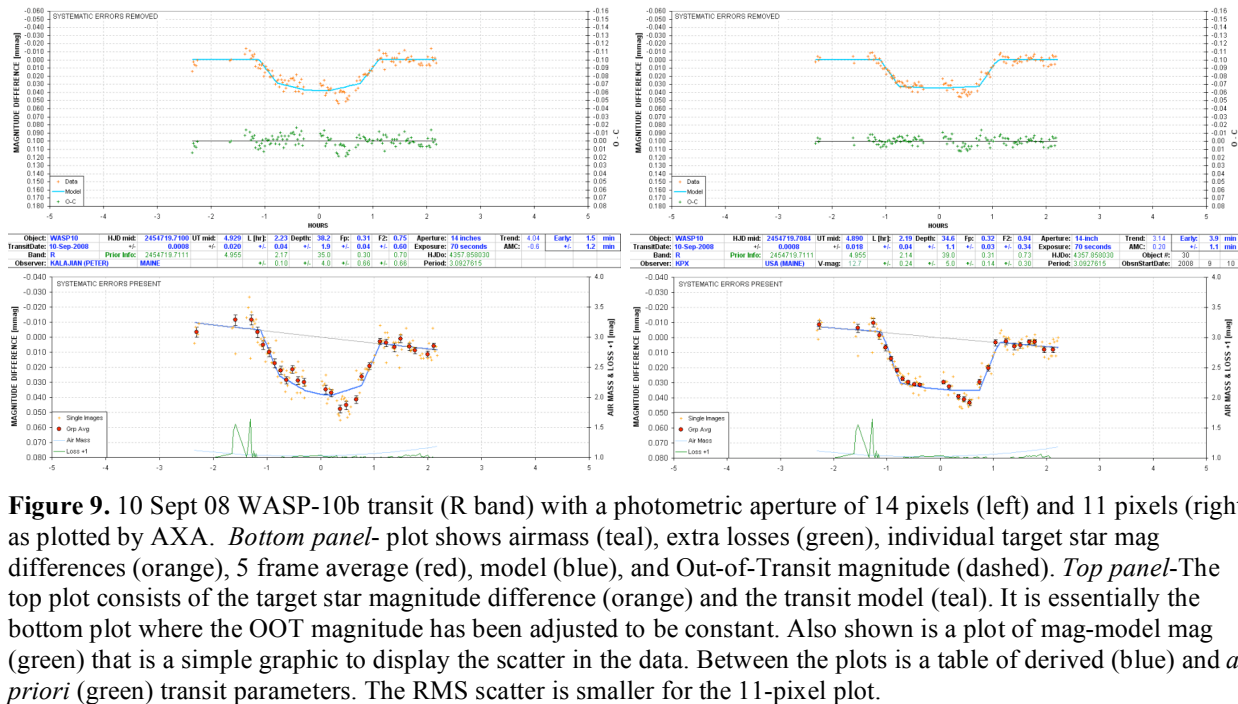


Figure 10. 8 October 08 WASP-10b transit (clear filter) with photometric aperture of 14 pixels (left) and 11 pixels (right). The RMS scatter is lower for the 14-pixel aperture.

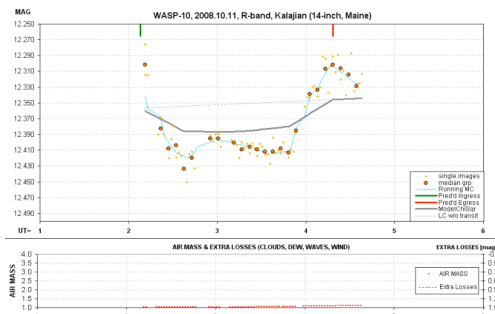


Figure 11. 11 October 08 WASP-10b transit with photometric aperture of 14 pixels. Poor photometric conditions have conspired to make the data suspect. This transit LC was not submitted to AXA.

3.4. Submission of Data to the Amateur Exoplanet Archive

One of the goals of this project was to submit transit data to the Amateur Exoplanet Archive (AXAWeb). This is a public domain archive of all of the bright transiting objects discovered so far. Amateur data can be submitted in tabular form consisting of time and extinction corrected magnitude of the target. If artificial star photometry has been used, the extra losses can also be submitted.

At this writing, the archive is maintained by Bruce Gary, but there are plans to move it to a professional academic repository by the end of 2008 (Personal communication, Gary 2008). Gary has written a series of data reduction programs to plot the data in a consistent manner. The transit plots are those generated by his automated plotting routine.

4. Discussion

4.1. Noise

No photometric project can ignore the presence of noise, and it is important to characterize and minimize it in order to get the best possible results. There are four primary noise sources in CCD photometry: Poisson noise, noise introduced by calibration, scintillation noise, and CCD readout noise (Castellano et al. 2004).

Since Poisson noise scales as $1/\sqrt{N}$, where N is the number of photo-electrons arising from a star in a given aperture, we need 10^6 of these in order to have noise less than one mmag. One way to determine N is to use the equation $S/N \sim \sqrt{N}$ (Howell 2006). For the 8 October transit, the transit star $S/N > 2000$ so $N \gg 10^6$. It follows that for the transit images, Poisson noise is less than 1 mmag.

Calibration noise can arise from careless flat fielding or poorly exposed dark frames. A 200-pixel aperture area of the flat field master combined frame includes $\sim 3 \times 10^6$ ADU's, limiting the flat field's Poisson noise contribution to < 1 mmag. My analysis of §3.11 seems to indicate that the flats have resulted in consistent background values across the image. I infer from this that pixel-to-pixel variations have been minimized.

Scintillation noise depends on various factors including telescope aperture, altitude of the observatory, airmass and integration time. Larger aperture telescopes with integration times > 45 seconds observing through small airmass should yield scintillation errors < 3 mmags (Castellano et al. 2004). The AAVSO online scintillation calculator (SCINweb) calculates values all less than 1 mmag for the duration of the October 8 transit.

Read noise is minimized as a function of total noise by increasing exposure length. At > 45 seconds, this component of noise is < 1 mmag. (Castellano et al. 2004)

From the above, it can be inferred that the total noise contribution should be on the order of ± 3 -5 mmags. Looking at the LCs it appears that the total noise contribution is on the order of ± 10 mmags. What accounts for this discrepancy? Figure 12 gives us some clues. Note that the RMS scatter varies with airmass. The RMS values stabilize at the theoretically predicted noise contribution for airmass < 1.075 . This suggests that the extra noise component might be due to scintillation, but the order of magnitude difference between theoretical and observed scintillation noise suggests that there are other factors involved.

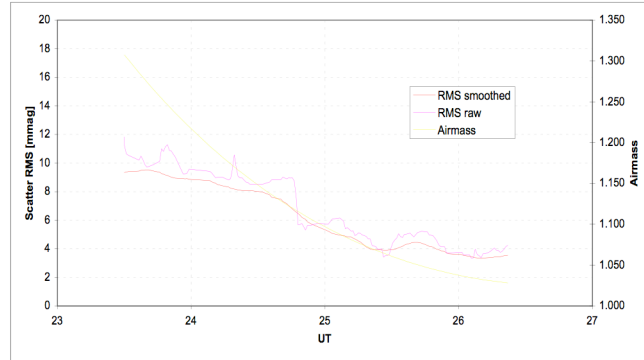


Figure 12. Scatter RMS and Airmass vs time for the 8 October transit (14 pixel aperture). Note the strong correlation. Note also the leveling out of the scatter below airmass 1.075 to the theoretically predicted total noise contribution.

Could the general downward trend of the noise partially be explained by the cooling of the optic? The 8 October transit occurred shortly after twilight, so the telescope was still cooling off from the day's heat. Visual observations have taught me that optical quality depends on the primary mirror being at or near ambient temperature. One measure of optical quality might be stellar FWHM. Does the FWHM improve as the optic approaches ambient? Might that have an impact on the noise? Figure 13 shows the trend of the FWHM over the course of the transit. There is a clear trend towards *larger* FWHM values, probably due to focus degradation from temperature-induced contraction of the OTA. This suggests that small changes to FWHM during the transit have little effect on the total noise.

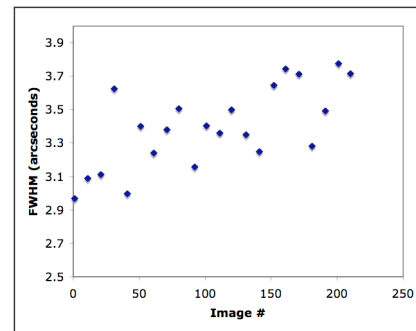


Figure 03. FWHM vs Image # for the 8 October transit. There is a clear upward trend for FWHM, probably due to degrading focus

Gary (Personal communication, 2008), suggests that the downward noise trend could be explained solely by field rotation due to polar alignment error. Even with perfect AO-8 behavior, where the guidestar stays on the same set of pixels, any polar alignment error (mine is ~ 6 arcminutes) will be seen as field rotation. If there is any error in the flat fielding, that could account for the change in RMS over time as stars wander across pixels.

In subsequent transit observations I intend to pay even closer attention to image calibration, AO-8 operation, polar alignment and signal to noise ratio. Figure 12 shows that it is possible to keep the RMS noise contribution below 5 mmags for my setup when everything is working well, so that's the goal for future observations.

4.2. Choosing Photometric Aperture

I initially used a photometric aperture of 14 pixels (diameter) for both transits. Comparing left and right plots in Figures 9 and 10, it is clear from the scatter that the choice of photometric aperture is of vital importance to the final quality of the light curve. As noted above, a good starting point is 3 x FWHM, but my data shows that decreasing aperture size below this value decreases the scatter in the data. Starting with the 3 x FWHM rule of thumb, I plotted the 10 September data for several apertures and chose that aperture that exhibited the smallest scatter. After empirically deciding on an 11-pixel (binned) diameter aperture, I used the aperture optimization tool from Mirametrics (MIRAweb) and found that this same aperture (shown as a radius of 5.5 pixels in Figure 14) theoretically leads to the smallest photometric error. The calculated photometric precision for this aperture with my camera and telescope is ~ 2.5 mmags.

I used the tool to model the 8 October data, and found that the same aperture led to a minimum magnitude error ~ 1.5 mmags, due to the use of a clear (vs. red for the 10 Sept. data) filter and shorter exposure time (45 vs 70 secs.) .

Unfortunately, things are never as tidy as the theory suggests. I redid the 8 October transit photometry with this theoretically optimized 11-pixel aperture, and the RMS scatter increased. The 14-pixel aperture was better for this dataset. For the purposes of submission to AXA, an iterative approach to aperture optimization is essential.

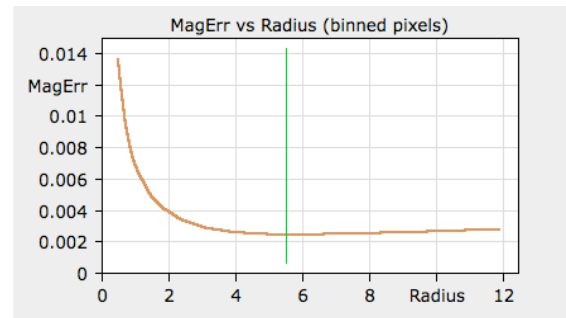


Figure 13. Magnitude error vs. photometric radius in pixels as modeled by the Mirametrics tool (MIRAweb). A radius of 5.5 yields the lowest magnitude error (~ 2.5 mmag). This optimized aperture radius compares well with my empirically derived optimal aperture.

4.3. Systematic Error

Recall the earlier discussion about color differences between target and check stars. It is clear from the bottom plots in figures 9 and 10 that there is an overall droop to the magnitudes as time goes on. Remember that these curves have been plotted after an extinction correction has been applied. What can be causing the droop? Since the extinction model arose from the sum of check star magnitudes, the model is going to be most accurate for stars that have an “average” color. By average, I mean one that combines all the check star colors. If the transit star has a color near this average, no droop, or airmass curvature will be seen in the magnitude plot. That my data exhibits this airmass curvature means that the target star is bluer than the average check star color and therefore is more affected by extinction.

The top plots of figures 9-10 simply apply an offset to each point. By noting the magnitude of the out-of-transit data points, a curve of best fit is applied as the baseline extinction. The offset is just the difference between this curve and the ideal (horizontal) OOT magnitude.

One can argue that this sort of offset correction is arbitrary, but since we’ve accounted for extra losses and some of the extinction already, if we assume that the OOT magnitude remains constant, it follows that over the short time period of the transit, the linear transformation is justified. There is no doubt that the ability to compare LCs visually is a powerful tool. Without the systematic correction, comparison would be difficult or

impossible. Removing the systematic error due to color differences is the norm in professional journal articles covering exoplanet transit LCs.

4.4. Model Fit

The AXA model is a simple one that tries to minimize the chi square RMS value of the difference between the data and the model by iterating values for the transit parameters F_2 , F_p , depth and length. This is an automatic process that treats all data equally, no matter the observer. In this way, observations from many different observers can be compared and trends in the parameters can be observed. A complete discussion of Gary's procedure can be found at <http://brucegary.net/AXA/Fitting/fitting.html>.

4.5. Transit Timing Variations

One of the most exciting aspects of amateur exoplanet work is the discovery of other planets in orbit around the same star as the known transiting planet. As noted in §1, transit-timing variations are an excellent way to infer the presence of another planet. Orbital dynamics between the star and planets will affect the orbit of the transiting star on short time scales. By monitoring the transit timing vs. time over the long term, these orbital changes should be visible. At this writing (October 2008), there have only been 4 transits of WASP-10b observed by amateurs, so nothing can be inferred about other planets in this system but other systems like HD 17156 are being actively monitored for transit-timing variations (Short et al. 2008). Amateurs are also doing interesting work at modeling these multiple star systems in conjunction with Greg Laughlin's Systemic program (SYSTEMICweb). Some of the data used for this modeling comes from the AXA.

5. Conclusion

This is an exciting time for the dedicated amateur astronomer who is interested in contributing to the professional scientific community. Using off-the-shelf astronomical equipment available at modest (<\$20k) cost, an amateur can obtain excellent transit light curves of known exoplanets with a little concerted effort. WASP-10 makes a good first target because of its relative brightness, proximity to similarly bright check stars, deep transit and newness. Observations in and out of transit will add to the small set of observations available at the AXA. Additionally, because of the size and eccentricity of the transiting planet, there is a good chance that other planets if present in the system will manifest themselves in the transit timing variations of WASP-10b. It is my hope that this paper will spur others to join this fledgling effort to observe exoplanets.

I wish to thank Jacob Gerritsen for his generous permission to use Galaxy Quest Observatory, and Bruce Gary for his patient mentoring and unstinting efforts to make me a better transit observer. AXA runs on his passion and enthusiasm.

Appendix 1

Although Bruce Gary's book (2008) is an excellent resource for prospective transit-observers, I think a succinct primer that enumerates the steps from preparation to acquisition to submission may be of interest. This is such a step-by-step guide.

1. Check your mount's polar alignment. Make sure that the error in both altitude and azimuth is less than 5 arcminutes if possible.
2. Check that your computer's clock is accurate. Synchronize it to one of the web-based time servers. This step is critical for transit timing variation studies.
3. Check the linearity of your camera. See Gary's book (2008) or my method as outlined in §3.1.2
4. Check the AXA website (<http://brucegary.net/AXA/x.htm>) and decide on a target. Download the BTE_ephem.xls spreadsheet from http://brucegary.net/book_EOA/xls.htm and find out the timing for the next transit of your target.
5. Using your favorite planetarium program, check the field around your target for the field of view of your telescope/camera. Adjust the rotation angle and field center to include your target and as many check stars of similar magnitudes as you can.
6. On a clear night before the transit, image the target star through your filter of choice at the maximum altitude that it will attain during the transit and decide on an exposure time that will keep the maximum pixel value well within the linear range of your detector. Try to balance signal to noise ratio with length of exposure. For the transit LC, shorter, more frequent images are desirable, but noise considerations require a S/N ratio > 1000. At the end of the run, rotate the camera to the desired PA for the transit and focus your telescope just before you shut it off.
7. On the day of the transit, make sure that you open your observatory roof or get the telescope outside well in advance of twilight so it begins to cool off. Consider making a diffuser of some sort so that you can get good quality sky flats at dusk. Your camera should be at the correct PA from step 5, and fairly well focused. Take 20 sky flats through the desired filter and then slew to the target. Focus, but don't rotate your camera or in any way displace it.
8. If you have an AO, get it calibrated and up and running. Begin the transit run. Expose for the exposure length you found out in step 5. Monitor your AO to make sure that you are autoguiding well.
9. Keep exposing until you are good and sure that the transit has completed, and then expose for another half hour or more to get a good post-transit magnitude baseline.
10. After the transit, take 20 darks and 20 bias frames at the same temperature as your science run. Take 20 more dawn flats and sigma-combine them with the dusk flats. Sigma-combine the darks and bias frames and calibrate your science images.
11. Go through each image and cull the ones that are not of the highest quality. Eliminate frames with poor guiding, obvious clouds, or other defects. Align the images and then insert the artificial star. Save the images to a new directory. These are your science images, ready for photometry.
12. Use MDL or other photometric reduction package to tag the artificial star, transit star, and as many check stars as you can and generate the photometry file. Save the data.

13. Using Gary's LC_x Template spreadsheet (available at the same website as in step 3.), import the photometry file into the "import AS" tab of the spreadsheet and delete the column that has the reference star magnitudes in it. Copy the data from all the remaining columns.
14. Paste the data into the "STD" tab starting in cell b11. Scroll down to the bottom of your data and delete all the rows below the last row of your data.
15. Switch to the "EXT" tab and scroll down to delete any rows of data below the ones you just imported, then adjust the axes of the Magnitude vs. Airmass graph to reflect your data. This is a graph of the sum of the fluxes of your check stars vs. airmass. You are going to fit the line on the graph to your data by adjusting the blue cells, g4 and g5, (and possibly g6 depending on your data: see Gary's instructions about this). Once the line fits your data as well as possible, you've got an extinction model that will be applied to the raw data to account for changes in airmass.
16. Adjust the axes of the Extra Losses graph to reflect your data. This graph shows you if there were changing photometric conditions during your run. If all went well, the extra losses should be near zero. Don't worry too much at this point if there are some extra losses. They will be deducted from the data on the next tab.
17. Now switch to the "m=0" tab and delete data below yours as above. Change the check star magnitude vs. time graph axes to reflect your data. Here's where you see if your check stars are well behaved. There are two graphs: the bottom one has the vertical scale exaggerated. Look at each check star in turn and note any that don't have constant magnitude as a function of time.
18. Scroll up to the blue cells in row 8 and change the 1's to 0's for any check stars that you don't want to use in the final magnitude calibration. The data in the columns below the 0's should disappear.
19. Scroll to the right until you see the block of orange cells. This is the data that you will upload to AXA. It consists of time, magnitude, and extra losses. Copy the entire block of numbers to the "import AXA" tab where the orange block is.
20. Edit the header for your location and details, and then copy the entire header and data into a text file. This text file is the file that you will send to AXA. Name the file "yyyymmdd-target_name-observer.txt"
21. Sit back and pat yourself on the back! Wait for Bruce to put your valuable contribution to science up on the web. Well done! Start planning for the next transit.

References

- Adams, F.C. & Laughlin, G. 2006, *ApJ*, 649, 992
 AOweb: SBIG AO-8, <http://www.sbig.com/sbwhtmls/ao8.htm> (accessed 8/28/08)
 AXAweb: Amateur Exoplanet Archive, www.brucegary.net/AXA/x.htm (accessed 8/25/08)
 BISQUEweb: Paramount ME, <http://www.bisque.com/Products/Paramount/> (accessed 8/28/08)
 Bissinger, R. 2007, *SASS*, 26, 17B
 Bonnarel, F., Fernique, P. & Boch, T. 2000, *A&AS*, 143, 33B
 Castellano, T., Laughlin, G., Terry, R. S., Kaufman, M., Hubbert, S., Schelbert, G. M., Bohler, D. & Rhodes, R. 2004, *JAAVSO*, 33, 1C
 Charbonneau, D., Brown, T. M., Latham, D. W. & Mayor, M. 2000, *ApJ*, 529L, 45C
 Christian, D.J. et al., 2008, preprint, (arXiv0806.1482C)
 Gary, B. 2008, *Exoplanet Observing for Amateurs*, self-published, available at http://brucegary.net/book_EOA/x.htm
 Howell, S. 2006, *Handbook of CCD Astronomy*, 2nd Edition, Cambridge University Press, Cambridge UK

LX200web: Meade LX200, <http://www.meade.com/lx200-acf/index.html> (accessed 8/28/08)
MAXweb: Maxim D/L, http://www.cyanogen.com/maxim_main.php (accessed 8/28/08)
Monet, et al. 2003, *APj*, 125:984-993
Pollacco, D., et al. 2006, *PASP*, 106, 1088
SBIGweb: Santa Barbara Instruments Group, <http://www.sbig.com> (accessed 8/20/08)
SCINweb: AAVSO Scintillation Calculator, <http://www.aavso.org/observing/programs/ccd/airmass.shtml>
(accessed 10/15/08)
Short, D., Welsh, W. F., Orosz, J. A. & Windmiller, G. 2008, preprint (arXiv0803.2935S)
SKYweb: The Sky Version 6.0, <http://www.bisque.com/products/thesky6/> (accessed 8/28/08)
ST2000web: SBIG ST2000XM, <http://www.sbig.com/sbwhtmls/st2000xm.htm> (accessed 8/28/08)
SYSTEMICweb: http://oklo.org/?page_id=33 (accessed 10/29/08)
WASPweb: Superwasp Group, <http://www.superwasp.org/index.html> (accessed 8/25/08)